

SOME APPLICATIONS OF PARTICLE-IN-CELL CODES TO PROBLEMS OF HIGH INTENSITY BEAMS*

W. B. HERRMANNSFELDT

Stanford Linear Accelerator Center

Stanford University, Stanford, California, 94305

The technique of using the “particle-in-cell” method was developed in the field of plasma physics [1]. Borrowed for problems of intense beams, it becomes an especially powerful tool because such problems frequently use single species “plasmas” and so pose a less severe requirement on the computer. We will look at several problems in which the PIC code method has been useful. The first is the classical Pierce gun in a transient or short pulse mode. Here the transverse beam optics is strongly affected by the time dependence of the current. The second is a study of high power klystrons searching for the source of an instability. The third is the high power rf source called the “lasertron” which is under development at SLAC. The interesting new development for the lasertron simulation is the introduction of a double gap output cavity for improved efficiency. The lasertron and klystron simulations are steady state solutions to rf problems with high-Q cavities. In order to limit the computation to a realistic time, these simulations use an external equivalent circuit which can communicate with the beam tunnel through ports placed at the locations of the rf cavities. Applications for electron beams generally require using a fully relativistic electromagnetic code such as MASK. In some applications, the computation can be speeded up by limiting the solution of the fields to the electrostatic conditions. This can be especially helpful if the degree of precision required demands very large numbers of macroparticles. As a last example, we will show the use of this technique for a problem involving emittance growth for a high intensity beam for heavy ion fusion.

* Work supported by the Department of Energy, contract DE – AC03 – 76SF00515.

*Presented at the Second International Conference on
Charged Particle Optics, Albuquerque, New Mexico, May 19-23, 1986*

Introduction

The purpose of this paper is to demonstrate the application of the "particle-in-cell" or PIC code method to problems of intense charged particle beams. The PIC code method is most powerful when applied to problems involving rapid transients, as in a pulsed beam, or with rf fields, as in a linac buncher or a klystron. These are problems for which the electrostatic gun program, that was the subject of my talk [2] at the conference in Giessen, gives only a poor first approximation.

The two most popular programs for this type of work are ISIS [3] and MASK [4]. Other programs, such as those by Haber [5] and by Hofmann [6], have been extensively used for specialized problems such as transport of non-relativistic intense heavy ion beams.

We will now conduct a sort of limited travelogue through a few problems that illustrate the PIC code method.

Pulsed Electron Gun

The Stanford Linear Collider (SLC) requires pulses of 50 GeV electrons and positrons, each with 5×10^{10} particles, to collide in a $1 \mu\text{m}$ radius spot. The SLC gun operates with 2 nanosecond pulses of about 17A and 150 kV. Because the 2 ns pulse length is long compared to the transit time across the gun, the peak current and maximum beam cross section can be calculated with the electrostatic gun code. However, an accurate estimate of the emittance in a pulse requires accounting for the transient effects that the rise and fall causes. The root mean square emittance of a pulse is found [7] by summing over all particles:

$$\epsilon = \frac{4\pi}{\sum I_i} \left[\langle x^2 \rangle \langle x'^2 \rangle - \langle xx' \rangle^2 \right]^{1/2}$$

where, for instance, $\langle x^2 \rangle$ is the sum of all the x^2 , or y^2 , values weighted by particle current I_i , and $x' = dx/dz$.

When this calculation is made by the electrostatic gun code, or by MASK for the middle portion of the pulse, the value found is $\epsilon \simeq 3\pi$ cm-mrad. However, when summed over the entire pulse, the MASK code finds $\epsilon = 10\pi$ cm-mrad.

Figure 1 shows the R-Z particle density plot from MASK at the point in time when the pulse current is a maximum. This can be compared to the gun program result shown in Fig. 2. In order to simulate the complicated shape of the Pierce focusing structure, we have used the profile of electric fields given along the line corresponding to the extension of the drift tube boundary. The numbers, put into MASK, accurately determine the form factor for the fields across the port. The form factor is obtained for the gun at full current, and is then assumed to be constant as a function of time. A small transient change of the form factor is thus ignored.

In Fig. 3, the front of the pulse is shown just arriving at the right hand boundary. By comparison with Fig. 1, it is apparent how much smaller the spot is, due principally to the absence of space charge at the front of the pulse. The trailing end of the pulse has a similarly sized cross section. In looking at the trail of macro particles from MASK, note that these are snapshots in time; the trajectories do not exactly follow the trails of macro particles.

50 MW Klystron

SLAC is presently replacing all 243 high power klystrons as part of the "energy upgrade project" for SLC. The new tubes will run at 65 MW for about 3.5 μ s. Throughout the early phase of production, the klystrons have exhibited a tendency to have an amplitude modulation at 10-20 MHz, superimposed on the rf pulse. It has generally been necessary to carefully adjust the solenoidal focusing field, especially the coil nearest the gun which bucks out field on the cathode, in order to get stable operation. Even so, virtually all production tubes to date must be run somewhat temperature limited in order to achieve stability.

The method by which MASK is used to calculate klystron gain and efficiency was developed by Simon Yu [8] and is being extended by Ken Eppley [9]. In sim-

ulations of the klystrons under conditions that agree with laboratory parameters, good agreement with gain and efficiency are found. Recently, Eppley has been able to show that electrons emitted from the edge of the cathode, and allowed to enter the gun through a one-millimeter-wide slot between the cathode and the Pierce electrode, can be found entering the fifth (penultimate) cavity of the klystron at a certain point in the rf period. In Fig. 4, we show the R-Z particle density plot of a klystron operating normally, with the input beam found using the gun program. The input to Fig. 4 was made assuming that all of the beam comes from the surface of the cathode. If, however, it is assumed that emission from the sides of the cathode is sufficient to form a virtual cathode at the aforementioned slot, then those electrons, which may comprise about 5% of the beam current, are the same ones that can be seen entering the penultimate cavity in Fig. 5.

The onset of this interception can be affected by various parametric adjustments, especially of the drive power and the solenoidal field strength. The simulations show significant interception at drive levels at or above saturation. These same operating conditions correspond to the onset of the instability that results in the amplitude modulation in production tubes that was described above. Thus we have strong circumstantial evidence that the interception in the fifth cavity is due to transverse optics problems and results in the instability.

The Lasertron

As part of the search for rf power for a TeV-range collider of the future, we have an R&D project at SLAC to make a "lasertron". This is an rf source using only an rf modulated light beam and a photodiode to make current pulses which then pass through an rf output gap, similar to the output gap in a klystron. In an effort to improve the efficiency of this device, we have turned to using a double output gap, such as was used on an earlier project for a 150 MW klystron [10]. In Fig. 6, we show the R-Z particle density plot for the double gap lasertron. Because of the short bunches, which are now much shorter than the anode-

cathode gap, it is not necessary to use a traditional Pierce electrode. With this configuration, calculated efficiencies as high as 76% have been found for a design capable of ~ 35 MW of rf power. Values for the complex impedance of the two cavities, including the connecting slot, are found from the MASK output.[11]

Quadrupole Transport with Nonlinearities

One final example in this travelogue is included here partly just to show that the PIC code method may be applied very effectively in very different ways for different applications. We refer to the published [12] work by Celata using the 2-D PIC code SHIFT developed by Haber [5]. Here the problem is growth of emittance in an intense nonrelativistic heavy ion beam with quadrupole focusing.

Figure 7 shows a set of scatter plots of macroparticles in phase space and configuration space. External fields are applied simulating an array of electrostatic quadrupoles, including drift spaces and even 3-D end effects of the quadrupole elements. By doing the calculation in the beam's coordinate space, and assuming a long pulse, it is possible to have all of the particles in a 2-D projection. The purpose of these calculations is to find even the smallest hint of phase space growth that could become serious for a very long transport system. In particular, there was concern about image forces as the beam coherently moves about the centerline of the transport system. It was found, for imperfectly steered beams, that the image force caused significant emittance growth. Figure 8 shows the results from the distribution of Fig. 7 for a beam with a displacement in the x-direction. With the aid of the PIC code results, it was possible to find an especially satisfying solution to this problem. The simulations showed that nonlinearities due to image forces were more significant than other nonlinearities having to do with electrode spacing and dimensions. Note that this system is designed to transport an array of multiple beamlets, so that it is desired to use round electrodes which can serve to focus beamlets on up to four sides of each electrode. Changing the radius of the electrodes changes the size of a small dodecapole term in the field description. It was found that for a particular choice of electrode radius, the

emittance growth due to steering errors, was substantially reduced.

Conclusion

The PIC code method is a powerful tool which can be applied to many problems of charged particle optics. We have not attempted to be comprehensive, either to credit the developers of these codes, or to illustrate many of the ways in which the method can be used. Rather, we have chosen a few applications within our own experience in which significant results have been found.

Acknowledgements

At the risk of omitting people who have made valuable contributions to this project, I will at least try to acknowledge some whom we couldn't have done without. At the top of the list are the pioneers of the PIC method; Oscar Buneman, Ned Birdsall, John Dawson and their many coworkers. Then there are my coworkers, Harold Hanerfeld and Ken Eppley, and the support here at SLAC from many people, but especially Perry Wilson, Roger Miller and Matt Allen's Klystron Task Force. Much of the inspiration for applying this method to problems of electron accelerators came from Les Thode at LANL. Simulations looking for causes of emittance growth due to space charge effects in a linac were performed by Lapostolle [13]. The extension of these ideas for problems of intense beam transport for Heavy Ion Fusion was pioneered by Ingo Hofmann and Irving Haber. Thanks are due them and also to Christine Celata who continues the heavy ion work at LBL and provided illustrations for this paper. Adam Drobot and his team at Science Applications International Corp., have provided us with absolutely essential support for MASK. Thanks also to the computer people, especially everyone concerned with the Energy Research CRAY X-MP at the National Magnetic Fusion Computation Center. We continue to be stimulated by discussions with our consultants, especially Simon Yu, who invented the algorithms for the klystron simulations, and our two emeritus professors, Marvin Chodorow and Bernard Lippmann.

References

1. For reviews of this subject, the reader is referred to; J. M. Dawson, Particle Simulations of Plasmas, Rev. Mod. Physics 55, (1983) 403, and also to the book; Plasma Physics via Computer Simulation, C. K. Birdsall and A. B. Langdon, McGraw-Hill, 1985.
2. W. B. Herrmannsfeldt, Nuclear Instruments and Methods 181 (1984) 1208.
3. G. Gisler, M. E. Jones and C. M. Snell, Bull. Am. Phys. Soc. 29, (1984) 1208.
4. A. Palevsky and A. T. Drobot, Proc. Ninth Conference on Numerical Simulation of Plasmas, Northwestern Univ., Evanston, IL (1980), PA-2.
5. I. Haber, IEEE Trans. Nuclear Sci. NS-26, (1979) 3090.
6. I. Hofmann and I. Bozsik, Proc. 1981 Linear Accel. Conf. (1981) 116.
7. I. Hofmann, Advances in Electronics and Electron Physics, Supplement 13C, Academic Press, (1983) 49.
8. S. Yu, "Particle In Cell Simulation of High Power Klystrons", SLAC/AP-34, Stanford Linear Accelerator Center, (1984).
9. K. R. Eppley, S. Yu, A. Drobot, W. B. Herrmannsfeldt, H. Hanerfeld, D. Nielson, S. Brandon and R. Melendez, IEEE Trans. Nuclear Sci., NS-32 (1985) 2903.
10. T. G. Lee, G. I. Konrad, T. Okazaki, M. Watanabe and H. Yonezawa, IEEE Trans. Plasma Science, PS-13 (1985) 545.
11. K. R. Eppley, "Optimization of a Lasertron Double Output Cavity," SLAC/AP-48, Stanford Linear Accelerator Center (1986).
12. C. M. Celata, V. O. Brady, L. J. Laslett, L. Smith and I. Haber, IEEE Trans. Nuclear Sci., NS-32 (1985) 3193.
13. P. M. Lapostolle, CERN-ISR/78-13.

Figure Captions

Figure 1. Particle plots, in R-Z space, for the SLC gun operating at about 17A and 150 KeV. The units on the plot are in meters. For peak beam current, as shown here, the emittance calculated by MASK is $\sim 3\pi$ cm-mrad.

Figure 2. The SLC gun as calculated by the electrostatic gun program with the same parameters as in Fig. 1. The field profile across the port in the MASK simulation is found from the gun program which has all of the boundary details. The units marked on the axes are mesh units where each mesh unit is one millimeter square.

Figure 3. The particle density plot in R-Z space during the pulse rise time. At this instant, the front of the pulse is just reaching the end of the gun region. When an entire 2 ns long pulse is passed through the emittance window, the emittance calculated by MASK is $\sim 10\pi$ cm-mrad.

Figure 4. Particle density plot in R-Z space for an SLC klystron. Slots in the upper surface show the location of ports for the six cavities. The most striking feature here is probably the realization that bunching in a high power klystron does not involve longitudinal compression of the electrons so much as it does involve radial stacking of the particles.

Figure 5. The SLC klystron, under the same conditions as in Fig. 4, except for the addition of a source of electrons from the side wall of the cathode. These electrons can be shown (using color graphics) to be the same ones that are seen here entering the penultimate cavity.

Figure 6. The particle density plot in R-Z space for the double output cavity lasertron. Ports for the output cavities are illustrated by the short gaps in the beam tube. The beam tube is 14 mm in radius at the narrowest point. The photocathode is about 15 mm in radius, and is mounted on the face of the

cathode support structure which is shown on the left. The double output cavity allows selectively phasing the first gap to extract some energy from the bunch and enhance the bunching so that the second gap is more efficient. The result is expected to be efficiencies at $\sim 70\%$ during operation.

Figure 7. Phase space and configuration space plots from a quadrupole transport system for a high intensity heavy ion beam. External focussing fields, including nonlinearities, are imposed on the beam in the beam's own coordinate reference frame. The beam is displaced in the x-coordinate in configuration space in order to simulate nonlinearities due to image charges. Without the image effect, there is essentially no discernable emittance growth.

Figure 8. Emittance growth, as a function of distance, for the heavy ion beam shown in Figure 7. After an initial jump, which is probably a result of the particles naturally adjusting the initial distribution, there is a small continuous growth. It was found possible to prevent this growth with the right choice of radius for the quadrupole electrodes.

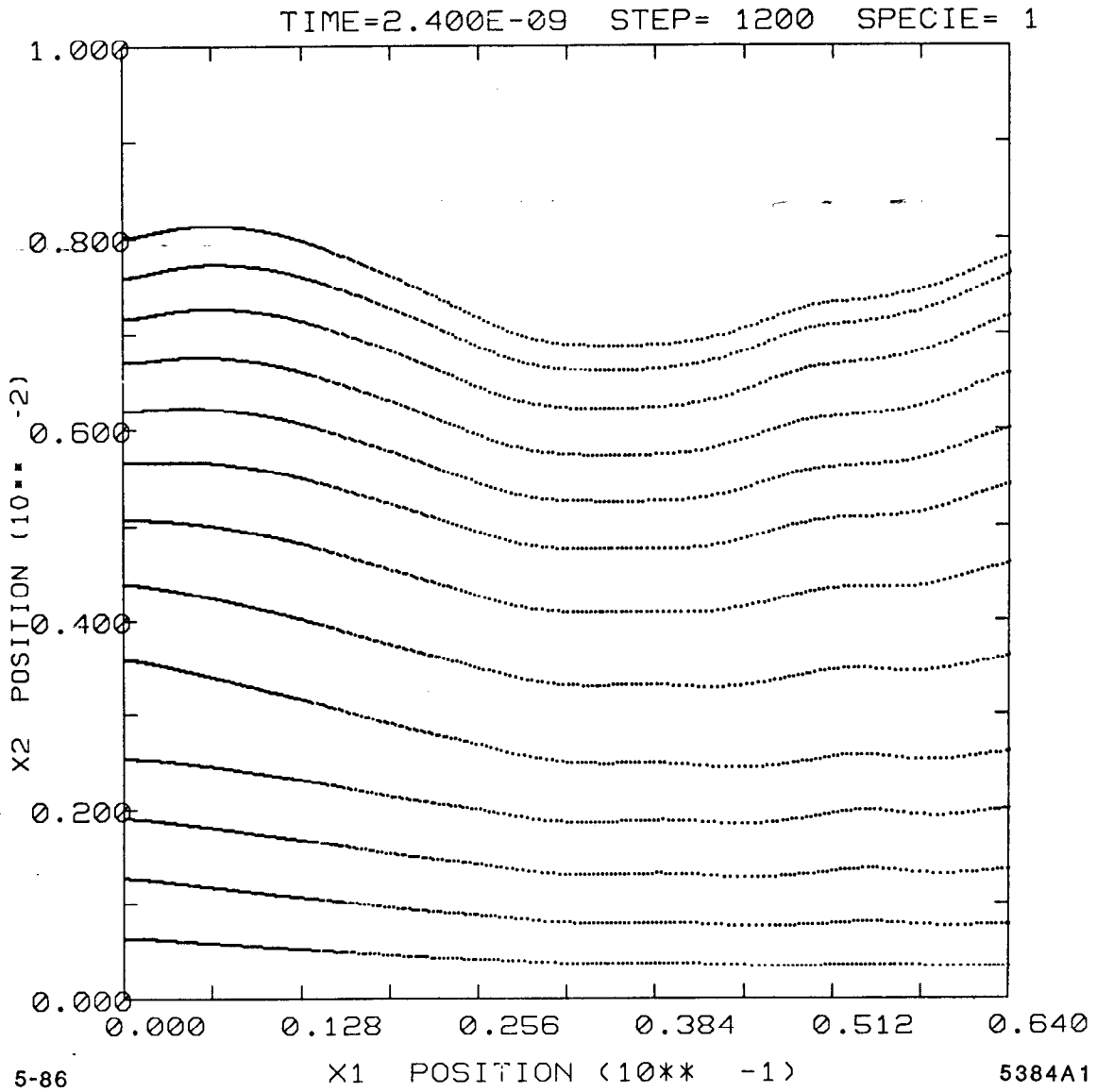
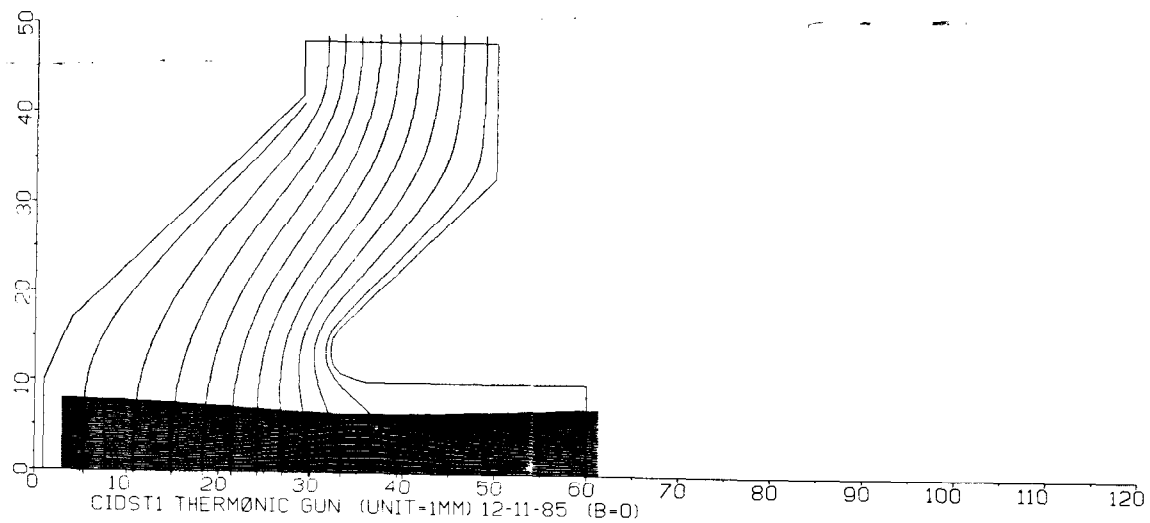


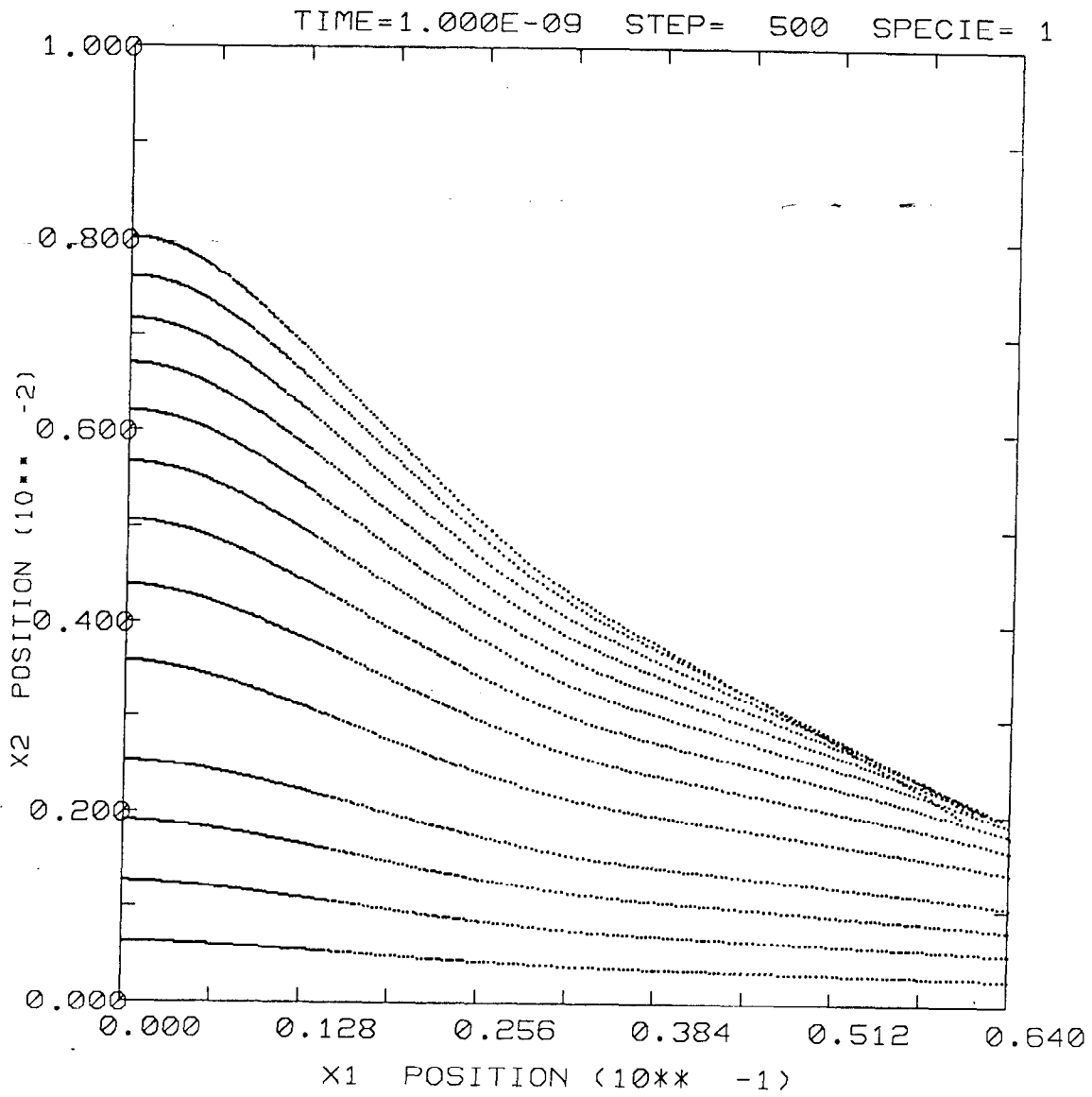
Fig. 1



5-86

5384A2

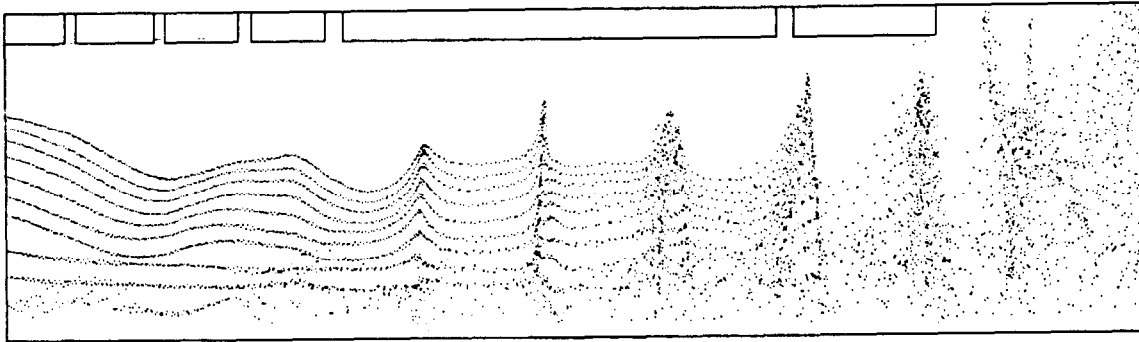
Fig. 2



5-86

5384A3

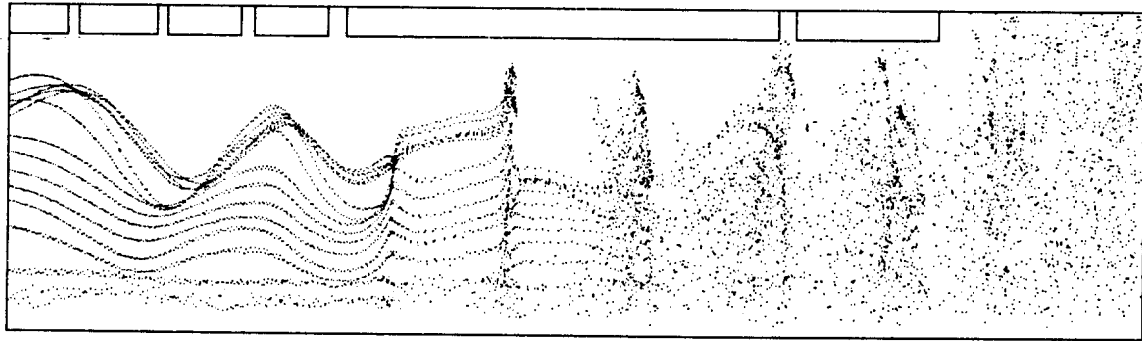
Fig. 3



5-86

5384A5

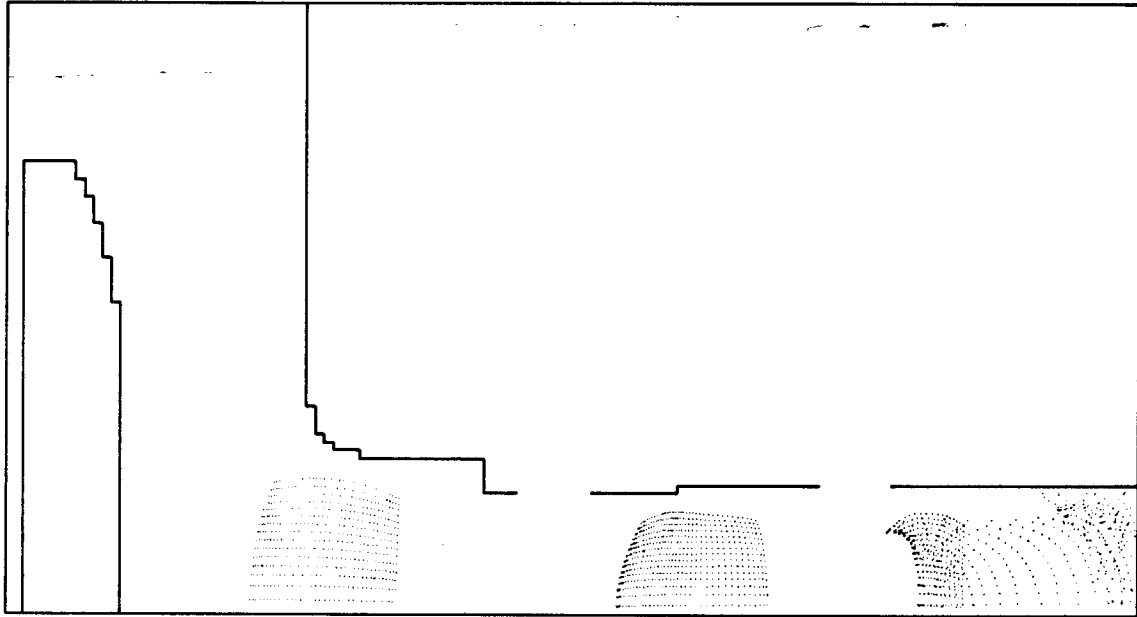
Fig. 4



5-86

5384A4

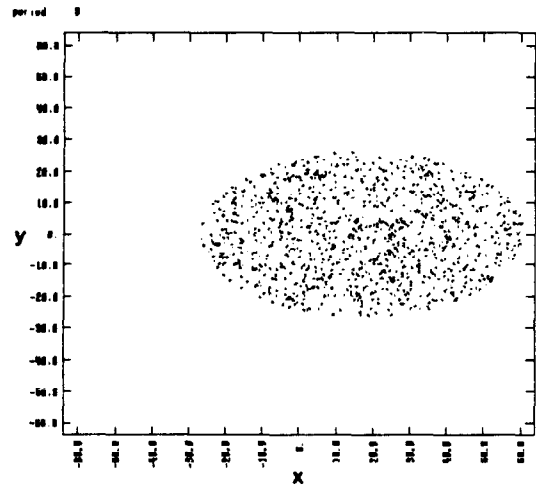
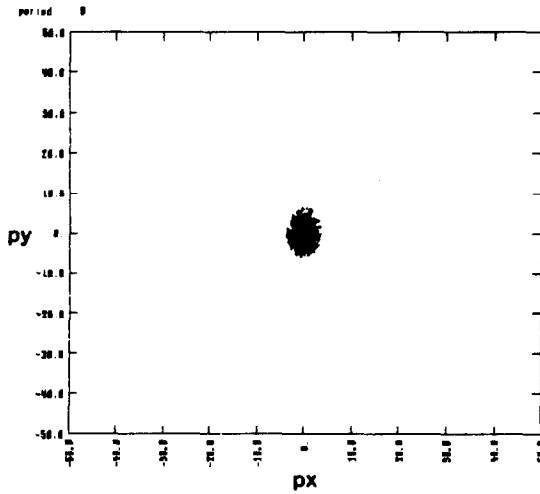
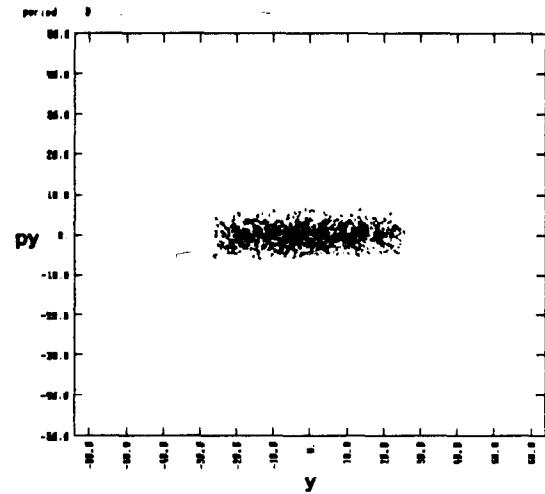
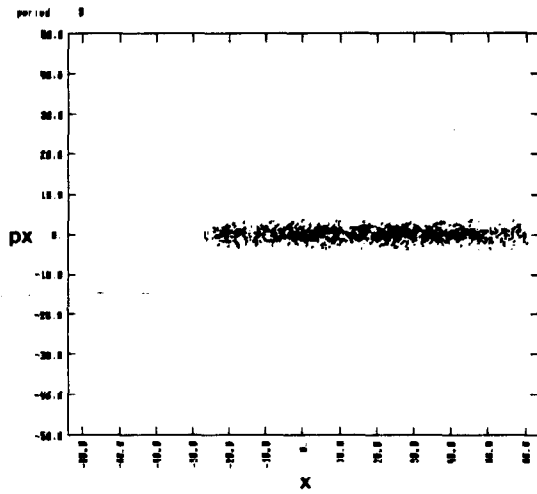
Fig. 5



2-86

5336A2

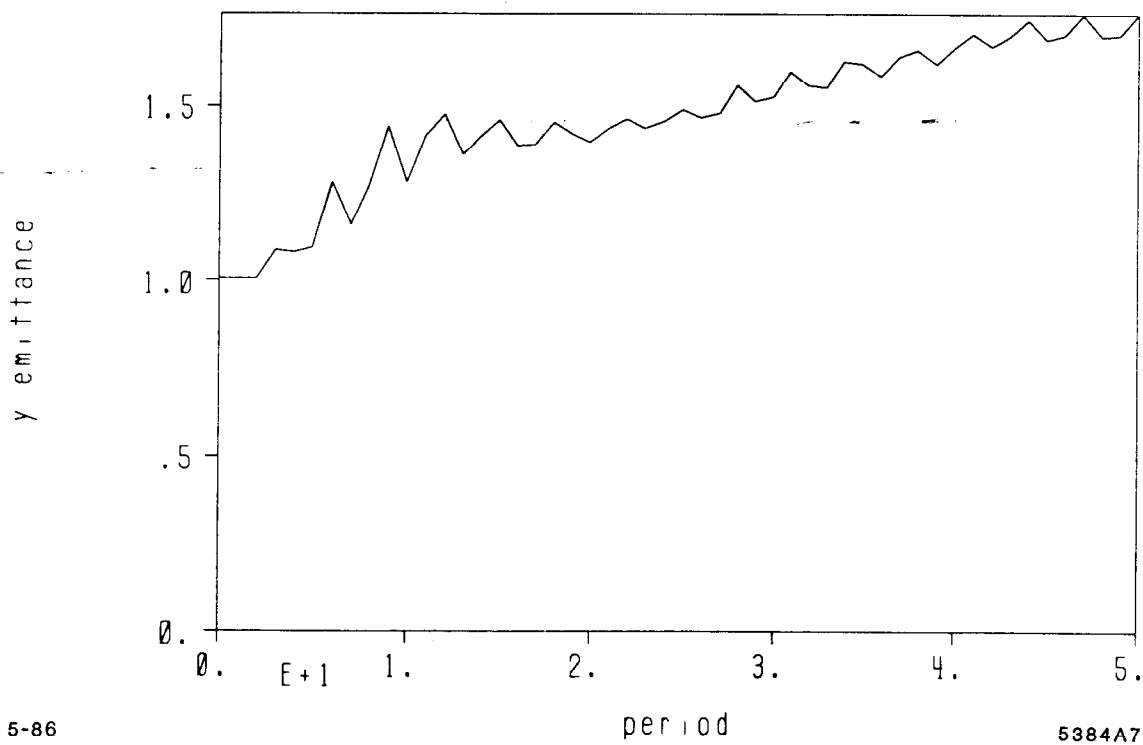
Fig. 6



5384A6 4-86

XBL 854-2325

Fig. 7



5-86

5884A7

XBL 854-2273

Fig. 8